Spectral technique for measuring phase retardation of a wave plate

Wei Wang (王 伟)*, Jianzhong Chen (陈建中), and Zhongbo Liu (刘中波)

Shandong Jiaotong University, College of Science, Changqing University Science & Technology Park, Jinan 250357, China

**Corresponding author: wwangsl@sdjtu.edu.cn*

Received August 3, 2014; accepted October 24, 2014; posted online January 5, 2015

We present a technique and algorithm for measuring the phase retardation of a wave plate based on spectral transmission curve. Through accurately extracting the intersection points' wavelengths from the spectral transmission curve, the effective phase retardation, absolute phase retardation, order, and physical thickness of the wave plate can be measured simultaneously in a wide spectral range. Experimental results show that the proposed technique has many advantages, such as higher data utilization, simpler extraction algorithm, and no strict requirement for the directions of transmission axes of the polarizer and analyzer, and the fast axis of the wave plate.

OCIS codes: 260.5430, 260.1440, 300.6190, 120.5410.
doi: 10.3788/COL201513.012601.

Wave plates are widely used as phase retardation devices in polarimetry, optical communication, laser modulation and optical measurement techniques, etc., and have become one of the most basic optics elements in modern optics[1,2]. The phase retardation of a wave plate is the most essential and important optical parameter because the accuracy of the phase retardation will affect the performances of the optical instrument employing the wave plate. To achieve a desired phase retardation of δ_0 ($0 \le \delta_0 < 2\pi$), wave plates can be designed as two types, zero-order wave plate with the phase retardation of δ_0 or multiple-order wave plates with the phase retardations of $\delta = \delta_0 + 2m\pi$, where $m = 1, 2, 3, \ldots$. For the multiple-order wave plates, m is called the order of the wave plate, δ and δ_0 are called the absolute phase retardation and effective phase retardation.

Naturally occurring crystalline materials, such as mica, calcite, and quartz, have traditionally been the birefringent materials of choice for wave plate. The thickness of a zero-order wave plate is so thin (less than 0.1 mm) and fragile, particularly for strongly birefringent materials such as calcite and quartz. It is very difficult to cut and polish a wave plate to such thickness especially for short-wavelength light. Due to its natural cleavage, mica can produce zero-order wave plates, but zero-order mica wave plates suffer from spatial nonuniformities and other difficulties[3]. So multiple-order wave plates are employed in most cases. Multiple-order wave plates have the main disadvantage of the phase retardation that shows more obvious temperature, angle of incidence dependencies compared with zero-order wave plates. In the same time, manufacture tolerance of the wave plates will result in an amplification of the phase retardation error. So the phase retardation values of many wave plates are not exactly nominal values, that is, a quarter-wave plate is not exactly $\pi/2$, a half-wave plate is not exactly π. When a multiple-order wave plate is used, the influence of ambient temperature fluctuation and stress–strain on the phase retardation should be taken into account, so it is necessary to measure the phase retardation of the wave plate before using it, including the absolute phase retardation and effective phase retardation, especially for the light is obliquely incident onto the wave plate[4]. And consequently, a reasonable, precise, and simple measurement method is needed.

Several effective methods have been developed to measure the phase retardation of a wave plate[4–14]. Relatively speaking, there are few methods that can perform simultaneous measurements of the absolute phase retardation and effective phase retardation of a wave plate[15–19]. Because all polarization information is contained in the spectral measurement[20], Feng *et al.* presented a method for measuring the thickness and phase retardation by judging the wavelengths of extremum points[18]. In fact, near the extreme value points of the spectrum curve, the slope of curve is close to zero, so it is difficult to obtain the wavelengths of extremum points accurately. It can lead to considerable errors in measurement results. Wang reported a method for determining the retardation through finding intersection points' wavelengths of two orthogonal spectral transmission curves[19]. The major shortcoming of this method is the need to measure spectral transmission for two times to produce the intersections. The complicated measurement procedure can lead to increased opportunity for errors. To overcome above shortcomings, in this letter, we develop a generalized technique and algorithm to accurately measure the optical parameters of a wave plate, including the absolute phase retardation, effective phase retardation, order, and physical thickness. We also systematically analyze the influences of the polarizer, analyzer, and wave plate azimuth angles. The analysis indicates that the proposed

 © 2014 Chinese Optics Letters

technique has no strict requirement for the directions of transmission axes of the polarizer and the analyzer, and the fast axis of the wave plate. This technique has the advantages such as higher data utilization, simpler extraction algorithm, easier operation, and higher measurement accuracy which are especially attractive when the phase retardation of a multiple-order wave plate accurate measurement in a wide spectral range is required.

The optical configuration for the measurement of phase retardation is shown in Fig. 1. The wave plate to be measured is placed between a polarizer and an analyzer, often known as Solc filter. The light beam passes successively through the polarizer, the wave plate, and the analyzer. Without loss of generality, assuming that the analyzer oriented at an arbitrary angle of α with respect to the polarizer, the wave plate with a phase retardation of δ whose fast axis making an angle of φ with the polarizer and the intensity of the input light is $I_0 = E^2$. Based on matrix optics theory, the Jones vector of the output light is given by

$$E = \begin{bmatrix} E_x \\ E_y \end{bmatrix} = M_A M_W M_P \frac{1}{\sqrt{2}} \begin{bmatrix} E_0 \\ E_0 \end{bmatrix}$$
$$= \begin{bmatrix} \cos^2\alpha & \sin\alpha\cos\alpha \\ \sin\alpha\cos\alpha & \sin^2\alpha \end{bmatrix} \begin{bmatrix} \cos\frac{\delta}{2} + j\sin\frac{\delta}{2}\cos 2\varphi & j\sin\frac{\delta}{2}\sin 2\varphi \\ j\sin\frac{\delta}{2}\sin 2\varphi & \cos\frac{\delta}{2} - j\sin\frac{\delta}{2}\cos 2\varphi \end{bmatrix} \begin{bmatrix} 1 & 0 \\ 0 & 0 \end{bmatrix} \frac{1}{\sqrt{2}} \begin{bmatrix} E_0 \\ E_0 \end{bmatrix}$$
$$= \frac{E_0}{\sqrt{2}} \begin{bmatrix} \cos^2\alpha\cos\frac{\delta}{2} + j\cos\alpha\sin\frac{\delta}{2}\cos(\alpha - 2\varphi) \\ \sin\alpha\cos\alpha\cos\frac{\delta}{2} + j\sin\alpha\sin\frac{\delta}{2}\cos(\alpha - 2\varphi) \end{bmatrix}, \quad (1)$$

where M_P, M_W, and M_A are the Jones matrices of the polarizer, wave plate, and analyzer, respectively. At a wavelength of λ the phase retardation of δ can be expressed as $\delta(\lambda) = \frac{2\pi d \Delta n(\lambda)}{\lambda}$, where d is the physical thickness of the wave plate, $\Delta n(\lambda)$ is the material birefringence at the wavelength of λ and also known as birefringence dispersion relation. Different birefringent crystals have different birefringence dispersion relations. The birefringence $\Delta n(\lambda)$ of any birefringent crystal, say A, can be represented in terms of power series of wavelength as[21–24]

$$\Delta n_A(\lambda) = \Delta_{0A} + \Delta_{1A}\lambda + \Delta_{2A}\lambda^2 + \cdots\cdots, \quad (2)$$

where Δ_{0A}, Δ_{1A}, and Δ_{2A} are the dispersion coefficients characterizing the birefringence of crystal A. Dispersion coefficients of the birefringence of the most used birefringent crystals can be obtained from Ref. [21].

From Eq. (1), the output light intensity $I(\lambda)$ is

$$I(\lambda) = E^{\dagger}E = \frac{I_0}{2}\left(\cos^2\alpha\cos^2\frac{\delta(\lambda)}{2} + \sin^2\frac{\delta(\lambda)}{2}\cos^2(\alpha - 2\varphi)\right). \quad (3)$$

So the transmission $T(\lambda)$ is expressed as

$$T(\lambda) = \frac{I(\lambda)}{I_0} = \frac{1}{2}\left[\cos^2\alpha\cos^2\frac{\delta(\lambda)}{2} + \sin^2\frac{\delta(\lambda)}{2}\cos^2(\alpha - 2\varphi)\right]. \quad (4)$$

Supposing that spectral range is from 400 to 800 nm, $\alpha = 0°$ and $\varphi = 45°$, in Eqs. (2) and (4), then theoretical normalized spectral transmission curve of a 600 μm thick quartz wave plate is obtained (Fig. 2). At the same time, a straight line represents that spectral transmission is equal to a certain constant (Fig. 2; e.g., 45%, which is only an example, but can also be other values as long as to ensure that the

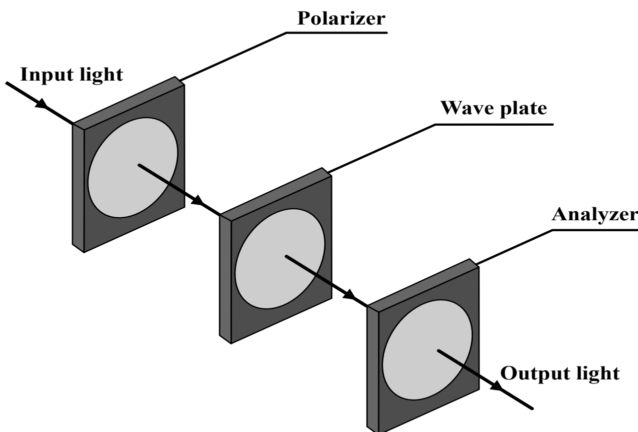

Fig. 1. Schematic diagram of the measuring system.

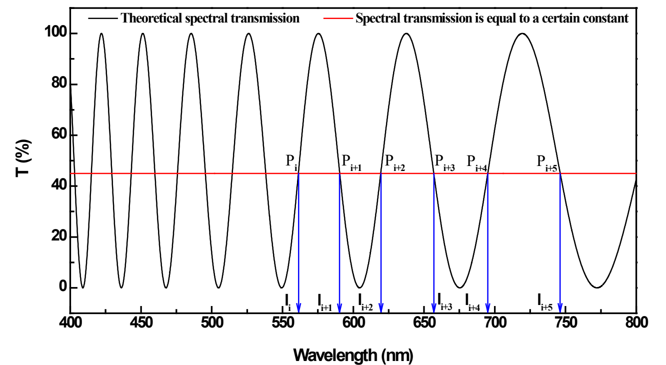

Fig. 2. Theoretical spectral transmission curve of a 600 μm thick quartz wave plate ($\alpha = 0°$, $\varphi = 45°$).

intersection points can exist). The spectral transmission curve and the straight line form a series of intersection points (denoted as P_i, P_{i+1}, P_{i+2}, P_{i+3}, P_{i+4}, P_{i+5},..., and corresponding wavelengths are λ_i, λ_{i+1}, λ_{i+2}, λ_{i+3}, λ_{i+4}, λ_{i+5},...). At the intersection points, the spectral transmissions are equal, the phase retardation of the wave plate at the intersection points satisfy

$$\cos^2\alpha\cos^2\frac{\delta_i}{2}+\sin^2\frac{\delta_i}{2}\cos^2(\alpha-2\varphi) = \cos^2\alpha\cos^2\frac{\delta_{i+1}}{2}+\sin^2\frac{\delta_{i+1}}{2}\cos^2(\alpha-2\varphi). \tag{5}$$

Equation (5) can be simplified to

$$\left(\sin^2\frac{\delta_i}{2}-\sin^2\frac{\delta_{i+1}}{2}\right)\left(\cos^2(\alpha-2\varphi)-\cos^2\alpha\right)=0. \tag{6}$$

Considering $\varphi \neq 0°$ or $\varphi \neq 90°$ in the measurement process (as explained further below), we can obtain

$$\sin^2\frac{\delta(\lambda_i)}{2}=\sin^2\frac{\delta(\lambda_{i+1})}{2}. \tag{7}$$

Similarly, we can get

$$\sin^2\frac{\delta(\lambda_i)}{2}=\sin^2\frac{\delta(\lambda_{i+1})}{2}=,\cdots,=\sin^2\frac{\delta(\lambda_{i+5})}{2}=C. \tag{8}$$

According to the periodicity of sine function, we have

$$\frac{\delta(\lambda)}{2}=n\pi\pm\arcsin\sqrt{C}, \tag{9}$$

where $n = 0, \pm1, \pm2, \ldots$. For clarity, Fig. 3 shows the relative relationship among the angles of $\delta(\lambda)/2$ at the intersection points (P_i, P_{i+1}, P_{i+2}, and P_{i+3}). From Fig. 3, we can get the phase retardation values' difference at the two intersection points, with one intersection point interval (P_i and P_{i+2}, or P_{i+1} and P_{i+3}, or P_{i+2} and P_{i+4}, or P_{i+3} and P_{i+5}, etc., i.e., two intersection points with one intersection point interval. For simplicity, P_i and P_{i+2} is used to represent the two intersection points in the following) as

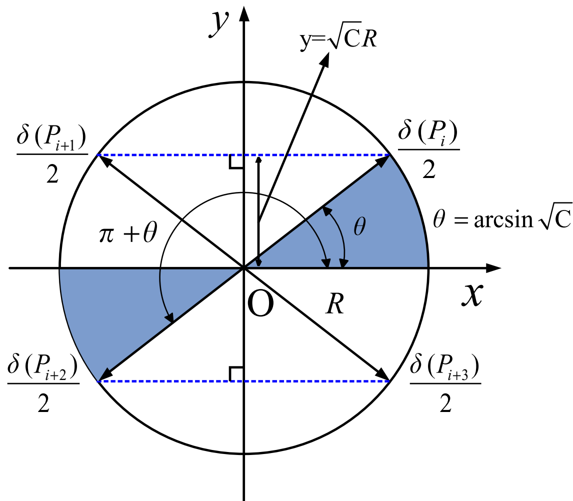

Fig. 3. Relative relationship between the values of $\delta(\lambda)/2$ at intersection points (P_i, P_{i+1}, P_{i+2}, and P_{i+3}).

$$\frac{\delta(P_i)}{2}-\frac{\delta(P_{i+2})}{2}=\frac{\delta(\lambda_i)}{2}-\frac{\delta(\lambda_{i+2})}{2}=\pi. \tag{10}$$

We obtain

$$\pi\frac{d\Delta n(\lambda_i)}{\lambda_i}-\pi\frac{d\Delta n(\lambda_{i+2})}{\lambda_{i+2}}=\pi. \tag{11}$$

So the physical thickness of the wave plate is

$$d=\frac{\lambda_i\lambda_{i+2}}{\Delta n(\lambda_i)\lambda_{i+2}-\Delta n(\lambda_{i+2})\lambda_i}, \tag{12}$$

where $\Delta n(\lambda_i)$ and $\Delta n(\lambda_{i+2})$ are the birefringences at the wavelengths λ_i and λ_{i+2}, respectively, which can be calculated by Eq. (2). So we can get the thickness of the wave plate by extracting the wavelengths at intersection points.

The absolute phase retardation of the wave plate at a wavelength λ_0 can then be expressed as

$$\delta(\lambda_0)=\frac{2\pi}{\lambda_0}\frac{\Delta n(\lambda_0)\lambda_i\lambda_{i+2}}{\Delta n(\lambda_i)\lambda_{i+2}-\Delta n(\lambda_{i+2})\lambda_i}, \tag{13}$$

where $\Delta n(\lambda_0)$ is the birefringence at the wavelength λ_0. The effective phase retardation of the wave plate at the wavelength λ_0 is

$$\delta(\lambda_0)_{\text{eff}}=\text{MOD}(\delta(\lambda_0),2\pi), \tag{14}$$

where MOD represents modulo operator. The order of the wave plate at the wavelength λ_0 is

$$N=\text{INT}(\delta(\lambda_0)/2\pi), \tag{15}$$

where INT represents the rounding function toward zero. Therefore, we can obtain the absolute phase retardation, effective phase retardation, order, and physical thickness of the wave plate by extracting the wavelengths of intersection points.

From the above derivation process, we can find that the expression of wave plate phase retardation is independent of the angles α and φ. That is, the optical parameter expressions of the wave plate (Eqs. (12)–(15)) remain valid for any angle α and φ as long as there exist intersection points. However, to extract the intersection points' wavelengths more accurately, the difference between the maximum and the minimum spectral transmission values of the spectral transmission curve should be as large as possible, which can reduce the influence of background light and stray light. To further evaluate the influence of the angles of α and φ on the spectral transmission value, Figs. 4(a)–(g) show the two-dimensional demonstration of a 600 μm thick quartz wave plate spectral transmission dependence on the angles of α and wavelength for different φ values. Figs. 4(h)–(i) show the spectral transmission for different φ values when $\alpha = 0°$ and $\alpha = 2°$, respectively. From Figs. 4(a) and (g), when $\varphi = 0°$ and $\varphi = 90°$, we can find that the value of spectral transmission is always a constant with the variation of wavelength for any angle α,

so in this case, there exist no intersection points. From Figs. 4(b)–(f), we can find that when $\varphi = 45°$ and for $\alpha = 0°$ or $\alpha = 90°$, the spectral transmission can vary from 0% to 100% with the variation of wavelength, that is, we can obtain the largest difference between the maximum spectral transmission and the minimum spectral transmission ΔT ($\Delta T = T_{max} - T_{min} = 100\%$). In other cases, as can be seen from Figs. 4(h) and (i), the value of ΔT is < 100%. Therefore, to reduce the measurement errors, in the actual measurements the angle of φ should be close to 45°. The angle of α should be close to 0° or 90°, that is, the polarizer is adjusted to near parallel or perpendicular to the analyzer, which can be accomplished by finding the maximum transmitted light intensity position or the extinction position. It should be noted that the angle of φ need not be strictly equal to 45° and α need not be strictly equal to 0° or 90°. In other words, in the process of adjusting the direction of the wave plate it allows for some misalignment.

By using error theory, based on Eq. (13), the maximum absolute error can be expressed as

$$\Delta\delta = \left|\frac{\partial\delta}{\partial\lambda_i}\right|\Delta\lambda_i + \left|\frac{\partial\delta}{\partial\lambda_{i+2}}\right|\Delta\lambda_{i+2}$$
$$= \frac{2\pi\Delta n(\lambda_0)}{\lambda_0}\left[\begin{array}{l}\dfrac{\Delta n(\lambda_i)\lambda_{i+2}^2}{\left(\Delta n(\lambda_i)\right)^2\lambda_{i+2}^2 - 2\Delta n(\lambda_i)\Delta n(\lambda_{i+2})\lambda_i\lambda_{i+2} + \left(\Delta n(\lambda_{i+2})\right)^2\lambda_i^2}\Delta\lambda_i \\ +\dfrac{\Delta n(\lambda_{i+2})\lambda_i^2}{\left(\Delta n(\lambda_i)\right)^2\lambda_{i+2}^2 - 2\Delta n(\lambda_i)\Delta n(\lambda_{i+2})\lambda_i\lambda_{i+2} + \left(\Delta n(\lambda_{i+2})\right)^2\lambda_i^2}\Delta\lambda_{i+2}\end{array}\right], \tag{16}$$

where $\Delta\lambda_i$, $\Delta\lambda_{i+2}$ represent the measurement errors, which depend on the resolution of spectrophotometer. Assuming that $\Delta\lambda_i = \Delta\lambda_{i+2} = \Delta\lambda$, $\Delta\delta$ is given by

$$\Delta\delta = \frac{2\pi\Delta n(\lambda_0)}{\lambda_0}\frac{\Delta n(\lambda_i)\lambda_{i+2}^2 + \Delta n(\lambda_{i+2})\lambda_i^2}{\left(\Delta n(\lambda_i)\right)^2\lambda_{i+2}^2 - 2\Delta n(\lambda_i)\Delta n(\lambda_{i+2})\lambda_i\lambda_{i+2} + \left(\Delta n(\lambda_{i+2})\right)^2\lambda_i^2}\Delta\lambda. \tag{17}$$

From Eq. (17), we can find that for a given material and wavelength λ_0, the item of $2\pi\Delta n(\lambda_0)/\lambda_0$ is a constant, so $\Delta\delta$ depends on two items,

$$f(\lambda_i,\ \lambda_{i+2}) = \frac{\Delta n(\lambda_i)\lambda_{i+2}^2 + \Delta n(\lambda_{i+2})\lambda_i^2}{\left(\Delta n(\lambda_i)\right)^2\lambda_{i+2}^2 - 2\Delta n(\lambda_i)\Delta n(\lambda_{i+2})\lambda_i\lambda_{i+2} + \left(\Delta n(\lambda_{i+2})\right)^2\lambda_i^2}$$

and $\Delta\lambda$. The function $f(\lambda_i, \lambda_{i+2})$ is a decreasing function of λ_i and λ_{i+2}, that is, $\Delta\delta$ decreases with an increase in intersection points' wavelengths. To reduce the measurement errors, we can choose intersection points of the spectral transmission curve in the long-wave band. At the same time, $\Delta\delta$ depends more on the $\Delta\lambda$ of the spectrophotometer resolution. Thus, we can improve the measurement accuracy by selecting the spectrophotometer with higher spectral resolution.

In order to demonstrate the feasibility of the proposed technique, a multiple-order quartz wave plate was measured. A UV-VIS spectrophotometer (UV-2550, Shimadzu Company, Japan) with a double light paths comparison system was adopted to measure the spectral transmission $T(\lambda)$ over the wavelength range from 400 to 800 nm. The optical schematic diagram of the proposed system is shown in Fig. 5. Light from a polychromatic light source passed through a monochromator and then the monochromatic light was divided into two beams by a beam splitter, one was the measuring light path and other was the reference light path. In the measuring light path, light passed successively through the polarizer, the wave plate (a half-quartz wave plate for 632.8 nm, Daheng Group Inc. China,) to be measured, and the analyzer. Then the light was incident on a detector, and the spectral transmission $T(\lambda)$ was obtained by comparing the light in the reference light path. The polarizer and the analyzer are Glan–Taylor prisms (Daheng Group Inc. China) with an extinction ratio of less than 10^{-5}, which can polarize the incident light in a wide spectrum. The polarizer, wave plate, and analyzer were mounted on rotation stages (Daheng Group Inc. China), respectively. With the rotation stages, the polarizer, wave plate, and analyzer can be rotated in vertical planes.

The polarizer, the analyzer, and the wave plate can be adjusted as follows. Firstly, the orientation of the polarizer and the analyzer was determined by adjusting the polarizer and the analyzer until a maximum intensity was obtained, which can be achieved by visual inspection. Considering the limited resolution of visual inspection, at this position, the polarizer

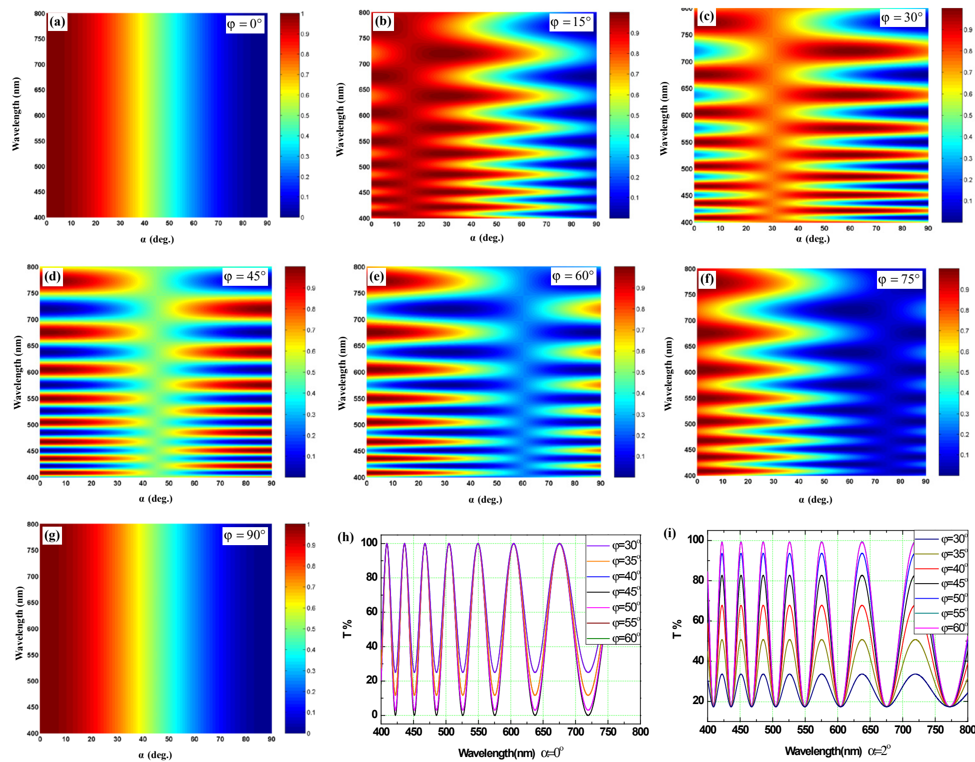

Fig. 4. (a)–(g) Two-dimensional demonstration of a 600 μm thick quartz wave plate spectral transmission dependence on the angles of α and wavelength and spectral transmission when (h) $\alpha = 0°$, and (i) $\alpha = 2°$.

and the analyzer were approximately parallel to the analyzer. Secondly, the polarizer and the analyzer were fixed in position and the wave plate to be measured was inserted between them. Then, the wave plate was rotated until a maximum intensity was obtained by visual inspection. At this position, the fast axis of the wave plate was approximately parallel or perpendicular to the analyzer. Finally, the wave plate was rotated by 45° either clockwise or counterclockwise. At this position, the fast axis made an angle of approximately 45° with the polarizer, that is, the angle of φ approximately equal to 45°. From the above adjustment process, we can find that the fast axis of the wave plate to be measured need not be known in advance.

After sufficient preheating of the spectrophotometer to ensure output spectrum is stable and choosing the highest resolution of 0.1 nm, the normalized spectral transmission $T(\lambda)$ is measured (Fig. 6). A straight line representing spectral transmission is equal to 45% is also given. Wavelengths at the intersection points are obtained with software (Fig. 6). Based on the wavelengths at the intersection points, in Eqs. (12)–(15), the thickness d, absolute phase retardation δ, effective phase retardation δ_{eff}, and the order (at 632.8 nm) of the measured half-quartz wave plate are calculated, respectively, and are listed in Table 1. It can be concluded that the measured average thickness of the measured wave plate is 455.340 μm, which coincides well with the value 455.23 μm given by the manufacturer. The average absolute phase retardation and effective phase retardation are 13.0030 and 1.0030π rad, respectively, and the measured wave plate is a sixth-order half-wave plate and the relative error is less than 0.4%. The wave plate acted as a

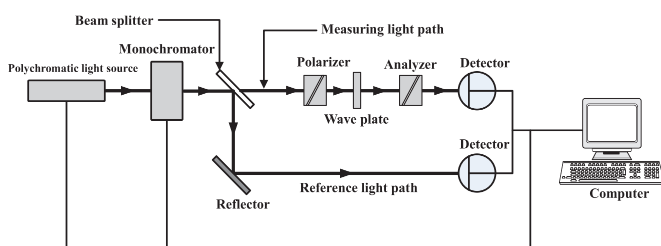

Fig. 5. Schematic diagram of the proposed system.

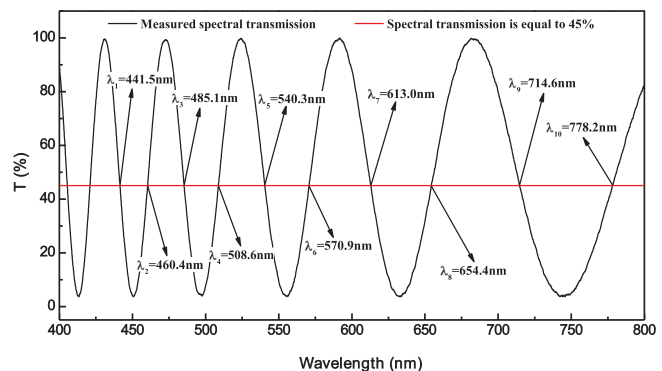

Fig. 6. Measurement results of spectral transmission curves of a half-quartz wave plate.

Table 1. Measurement Results of a Half-wave Plate at 632.8 nm

λ_i(nm)	λ_{i+2}(nm)	$d(\mu m)$	δ (rad)	δ_{eff}(rad)	E_r (%)
441.4	485.2	456.07	13.024π	1.024π	0.1850
460.3	508.7	456.10	13.025π	1.025π	0.1918
485.2	540.5	453.97	12.964π	0.964π	0.2783
508.7	570.9	453.95	12.963π	0.963π	0.2822
540.5	613.0	454.65	12.983π	0.983π	0.1290
570.9	654.4	456.07	13.024π	1.024π	0.1860
613.0	714.6	456.63	13.040π	1.040π	0.3090
654.4	778.2	455.28	13.001π	1.001π	0.0120
Average		455.340	13.0030π	1.0030π	0.1967

half-wave plate at 632.8 nm. Experiment results agree with the value given by the manufacturer. To further increase the data utilization and reduce the measurement errors, we can let the straight line represent other spectral transmission values, and obtain a series of other intersection points' wavelengths.

In conclusion, we present a technique and algorithm for simultaneous measurement of several optical parameters, including the absolute phase retardation, effective phase retardation, order, and the physical thickness of a wave plate. Experimental results demonstrate that the technique is effective. This technique has some advantages, such as higher data utilization, simpler extraction algorithm, better resolution and no strict requirement for the directions of transmission axes of the polarizer and the analyzer, and the fast axis of the wave plate. We believe that the technique reported here can be a useful approach for measurement of a wave plate.

This work was supported by the National Natural Science Foundation of China under Grant No. 11104164.

References

1. C. Zhang, L. Chai, Y. Song, M. Hu, and C. Wang, Chin. Opt. Lett. **11,** 051403 (2013).
2. H. Ye, Z. Gao, Z. Qin, and Q. Wang, Chin. Opt. Lett. **11,** 031702 (2013).
3. P. D. Hale and G. W. Day, Appl. Opt. **27,** 5146 (1988).
4. Z. P. Wang, Q. B. Li, Q. Tan, Z. J. Huang, and J. H. Shi, Opt. Laser Eng. **43,** 1226 (2005).
5. Y. L. Lo, J. F. Lin, and S. Y. Lee, Appl. Opt. **43,** 6248 (2004).
6. Y. L. Lo, C. H. Lai, J. F. Lin, and P. F. Hsu, Appl. Opt. **43,** 2013 (2004).
7. J. F. Lin, Opt. Commun. **281,** 940 (2008).
8. Y. Zhang, F. Song, H. Li, and X. Yang, Appl. Opt. **49,** 5837 (2010).
9. J. F. Lin, T. T. Liao, Y. L. Lo, and S. Y. Lee, Opt. Commun. **274,** 153 (2007).
10. K. Yang, A. Zeng, X. Wang, and H. Wang, Optik **120,** 558 (2009).
11. K. Yang, A. Zeng, X. Wang, F. Tang, and H. Wang, Chin. Opt. Lett. **6,** 673 (2008).
12. K. Yang, A. Zeng, X. Wang, H. Wang, and F. Tang, Chin. Opt. Lett. **6,** 568 (2008).
13. A. Zeng, F. Li, L. Zhu, and H. Huang, Appl. Opt. **50,** 4347 (2011).
14. R. Fang, A. Zeng, L. Liu, L. Zhu, and H. Huang, Chin. Opt. Lett. **10,** 091201 (2012).
15. S. Yoneyama, K. Nakamura, and H. Kikuta, Opt. Eng. **48,** 123603 (2009).
16. Y. T. Jeng and Y. L. Lo, Appl. Opt. **45,** 1134 (2006).
17. A. Safrani and I. Abdulhalim, Opt. Eng. **48,** 053601 (2009).
18. W. Feng, L. Lin, L. Chen, H. Zhu, R. Li, and Z. Xu, Chin. Opt. Lett. **4,** 705 (2006).
19. W. Wang, Opt. Commun. **285,** 4850 (2012).
20. F. Snik, T. Karalidi, and C. U. Keller, Appl. Opt. **48,** 1337 (2009).
21. P. Hariharan, Opt. Eng. **35,** 3335 (1996).
22. M. S. El-Bahrawi, N. N. Nagib, S. A. Khodier, and H. M. Sidki, Opt. Laser Technol. **30,** 411 (1998).
23. M. Emam-Ismail, Opt. Commun. **283,** 4536 (2010).
24. N. N. Nagib, S. A. Khodier, and H. M. Sidki, Opt. Laser Technol. **35,** 99 (2003).